Yunfei Xing
State Key Laboratory
of High Temperature Gas Dynamics,
Institute of Mechanics,
Chinese Academy of Sciences,
Beijing 100190, China
e-mail: xingyunfei@imech.ac.cn

Fengquan Zhong[1]
State Key Laboratory
of High Temperature Gas Dynamics,
Institute of Mechanics,
Chinese Academy of Sciences,
Beijing 100190, China
e-mail: fzhong@imech.ac.cn

Xinyu Zhang
State Key Laboratory
of High Temperature Gas Dynamics,
Institute of Mechanics,
Chinese Academy of Sciences,
Beijing 100190, China
e-mail: changxy@imech.ac.cn

Numerical Study of Turbulent Flow and Convective Heat Transfer Characteristics in Helical Rectangular Ducts

Three-dimensional turbulent forced convective heat transfer and its flow characteristics in helical rectangular ducts are simulated using SST k–ω turbulence model. The velocity field and temperature field at different axial locations along the axial direction are analyzed for different inlet Reynolds numbers, different curvatures, and torsions. The causes of heat transfer differences between the inner and outer wall of the helical rectangular ducts are discussed as well as the differences between helical and straight duct. A secondary flow is generated due to the centrifugal effect between the inner and outer walls. For the present study, the flow and thermal field become periodic after the first turn. It is found that Reynolds number can enhance the overall heat transfer. Instead, torsion and curvature change the overall heat transfer slightly. But the aspect ratio of the rectangular cross section can significantly affect heat transfer coefficient. [DOI: 10.1115/1.4028583]

Keywords: helical rectangular duct, heat transfer, turbulent flow, curvature, torsion

1 Introduction

Helical coiled ducts are widely employed as heat transfer exchangers in industrial applications such as power generation, nuclear industry, process plants, heat recovery systems, refrigeration, and food industry, because of their compact size and efficient heat transfer performance. It has been widely reported in literature that heat transfer rates in helical channels are higher as compared to that of straight ones [1]. Numerical or experimental studies on helical coiled channels with a circular cross section have been conducted. For example, Kao [2] theoretically and numerically studied the torsion effect on fully developed laminar duct flow in a helical pipe with constant circular cross section. The results indicated that the presence of torsion has large effects on flow field and heat transfer if the ratio of curvature to torsion is of order unity. Xin and Ebadian [3] tested five helical pipes with different torsions and curvature ratios to investigate local and averaged heat transfer characteristics. They found that the temperature distribution becomes fully developed after two turns from the inlet. The effect of torsion is very small in their test flow range. Ali [4] studied steady properties of natural convection heat transfer of helical coiled tubes with experiments. The results showed that heat transfer coefficient is enhanced either by reducing the diameter ratio (coil diameter to tube diameter ratio) or the number of coil turns. Wu et al. [5] investigated turbulent heat transfer in a helical coiled tube with larger curvature ratio. They found that the increase in wall friction and heat transfer coefficient due to the helical effect is smaller for the turbulent flow than for laminar flow. Many researches [6,7] focused on the parameter effect on the change of heat transfer coefficient of helical pipe and a power-law dependence of the averaged heat transfer coefficient has been proposed. Kaew-On et al. [8] studied the heat transfer of water flowing through the straight and helical minichannel tubes. The result shows that more enhanced heat transfer increase for tubes with greater curvature ratio. Mandal and Nigam [9,10] investigated on the pressure drop and heat transfer of turbulent flow in tube helical heat exchanger experimentally. The experiments were carried out with hot compressed air in the inner tube. They developed new correlations for friction factor and Nusselt number in the inner and outer tubes.

Although heat transfer and flow characteristics in a helical coiled channel have been studied for a few decades, it is worthy noticing that most of the previous studies are restricted to the heat transfer and flow of helical channels with a circular cross section. However, helical coiled channels with rectangular cross section are often used in cooling system for gas turbine, rocket engine, or scramjet applications [11–13]. Some studies about laminar flow in helical rectangular ducts have been reported [14–21]. But literatures of turbulent flow and heat transfer in helical rectangular ducts for the turbulent flow are very few. Mori et al. [22] studied forced convective heat transfer in a curved channel with a square cross section with both analytical and experimental methods. But the curved channel has only half turn, which is not able to represent typical effect of helical ducts with several turns. Therefore, the present work is to study turbulent heat transfer in helical ducts with rectangular cross sections with a few turns.

Another important issue is that the shape of the rectangular channel is critical for the enhancement of convective heat transfer and the associated studies are very limited. Therefore, in this paper, turbulent flow and heat transfer in helical ducts with varied rectangular geometries are investigated numerically and effects of key parameters such as Reynolds number, curvature and torsion, and the cross section of channel are discussed. The present work is expected to give insights into mechanisms of turbulent convective heat transfer in helical channels and provide references for engineering applications.

2 Geometry and Parameters of Helical Rectangular Duct.

Figure 1 shows a typical helical rectangular duct. The geometric parameters include width and height (a/b) of the duct, the curvature radius of the coil (R), and the coil pitch (p).

The dimensionless curvature and torsion can be defined as

$$\delta = \frac{a}{R} \tag{1}$$

[1]Corresponding author.

Contributed by the Heat Transfer Division of ASME for publication in the Journal of Heat Transfer. Manuscript received January 23, 2014; final manuscript received September 11, 2014; published online September 30, 2014. Assoc. Editor: Ali Khounsary.

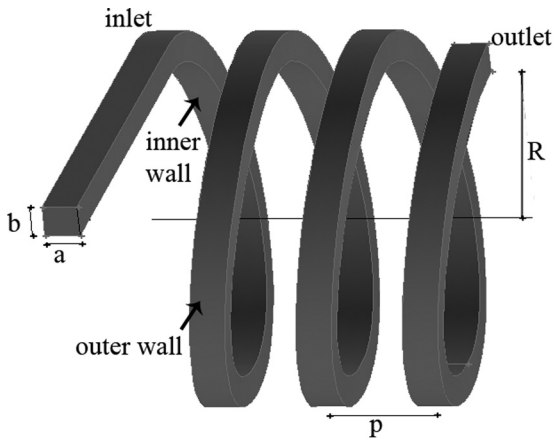

Fig. 1 Schematic diagram of a helical rectangular duct

$$\lambda = \frac{p}{2\pi R} \tag{2}$$

In the flow field we define Reynolds number, Nusselt number, and the friction factor as

$$\mathrm{Re} = \frac{2\rho u a b}{(a+b)\mu} \tag{3}$$

$$\mathrm{Nu} = \frac{2hab}{(a+b)k} \tag{4}$$

$$f = \frac{2 \cdot \Delta P \cdot d \cdot g}{l \cdot u^2} \tag{5}$$

where ρ is density, u is bulk velocity, h is heat transfer coefficient, l is the length of the duct, d is the hydraulic diameter, and ΔP is the pressure loss from inlet to outlet.

3 Numerical Method

3.1 Comparison With Experimental Heat Transfer Data. The accuracy of the present computation is also checked by comparing the heat transfer coefficient of turbulent air flow in a helical rectangular duct obtained with the present computation with different turbulent model and experiments reported previously by Mori et al. [22]. One can see that the turbulent model of SST k–ω can get a closer numerical result in Table 1, and $\mathrm{Nu_m}$ between the present numerical result and the experiment is only 9%.

Navier–Stokes equations are solved with finite volume method with shear stress transport (SST) turbulence model. The convective term is discretized by the second-order upwind difference scheme and the diffusion term is discretized with the second-order central difference scheme. The SIMPLE algorithm is employed to resolve the coupling between velocity and pressure.

For helical coiled tube, the critical Reynolds number judging whether the flow is laminar or turbulent is related with the coil curvature ratio and the relationship is given as follows [23]:

Table 1 Comparisons of fully developed Nusselt number with previous study with different viscous model with Reynolds number of 42,017

		Relative difference (%)
Mori et al. [22] Exp.	1549.2	—
Present study (k–ω)	1706.4	9
Present study (k–ε)	1712.3	9.5
Present study (Spalart–Allmaras)	1754.9	11.7

Table 2 Mesh parameters and grid independence results

Mesh	N_{SEC}	$\frac{\Delta r_{\max}}{\Delta r_{\min}}$	$y^+_{\min}$	h
1	3600	2.45	4.6	89445.3
2	6400	22	0.55	85682.8
3	9600	37	0.34	84627.3

$$\mathrm{Re_{cri}} = 2100(1 + 12\delta^{0.5}) \tag{6}$$

Since the range of Re studied in the paper is larger than the value of according to the largest curvature ratio, turbulent flow is studied.

3.2 Grid Independence. A grid-independence study has been carried out for the validation of the present numerical method. The three meshes used here are summarized in Table 2. Here, N_{SEC} is the total number of cells in the cross section, $\Delta r_{\max}/\Delta r_{\min}$ is the ratio of maximum to minimum cell sizes, and $y^+_{\min}$ is the first grid spacing from the wall normalized by the wall unit. It is worthy noticing that for accuracy simulation of turbulent heat transfer from the wall, $y^+_{\min}$ should be kept to be less than 1–2. The results of grid-independence study are reported in Table 1 for a helical and rectangular duct and typical values of curvature $\delta = 0.192$ and torsion $\lambda = 0.11$. There is a significant variation from mesh 1 to mesh 2 due to the refined resolution of the viscous sublayer of turbulent boundary layer. The difference of heat transfer coefficient is 1.2% for mesh 2 and 3. However, the computational time for mesh 3 is nearly two times higher than that of mesh 2. Therefore, mesh 2 is applied for all the simulations in the present study.

4 Results and Discussions

The helical rectangular duct has three turns (θ increases from $\theta_{\mathrm{i}} = 0$ deg at the inlet to $\theta_{\mathrm{o}} = 1080$ deg at the outlet) with a straight guide duct upstream of it as shown in Fig. 1. Water is selected as working fluid. The inlet temperature is 283 K, and the wall temperature is kept as 370 K. The inlet Reynolds number is 55,000, and the nondimensional curvature and torsion are 0.192 and 0.11, respectively.

4.1 Description of Velocity Field. Figure 2 presents the development of velocity field at different axial positions. Cross sections along the length of the coil are denoted by the angle (θ) measured from the inlet plane of the coil. At each position, the

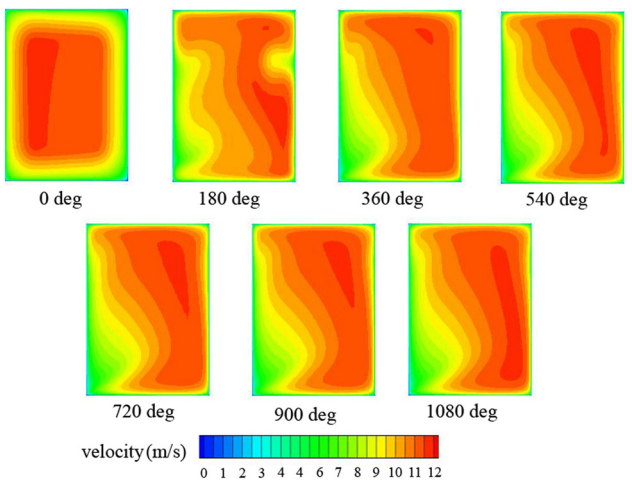

Fig. 2 Development of velocity field in varied cross sections along the axial direction ($\delta = 0.192$, $\lambda = 0.11$, and Re = 55,000)

left side is the inner wall, and the right side is the outer wall of the duct. It can be seen that the maximum axial velocity gradually shifts to the vicinity of the outer wall as θ increases. The curvature of the duct causes centrifugal force to act on the fluid, leading to a high-speed flow region near the outer side of the duct wall and a nonsymmetric velocity profile about the centerline of the duct. The figures indicate that as θ increases, the secondary flow is enhanced and convective heat transfer may be increased. When θ is smaller than 360 deg, the variation of velocity fields with increasing θ is more obvious, while θ is greater than 360 deg, no significant change can be found in the velocity field. The above findings show that an entrance region similar to that observed in straight channels exists also in helical ducts.

Figure 3 shows instantaneous streamlines in cross sections with varied axial positions. The significant secondary flow is clearly shown in the figures, which affects heat transfer rates in the outer and the inner walls of the duct. After one turn, which θ is greater than 360 deg, the streamlines show similarity. Note that some differences are found when θ is 1080 deg caused by the outlet boundary of the duct.

4.2 Description of Temperature Field. Figure 4 is the development of temperature field at different axial positions in the helical rectangular duct. At each position, the left side is the inner wall and the right side is the outer wall of the duct. There is negligible effect of secondary flow near the duct inlet. When θ is greater than 360 deg, a local high-temperature region is identified near the lower left corner of the duct where a low speed flow region exists as indicated in Fig. 2.

4.3 Description of Turbulence Intensities. Figure 5 presents the development of turbulence intensities at different axial positions. Cross sections along the length of the coil are denoted by the angle (θ) measured from the inlet plane of the coil. At each position, the left side is the inner wall, and the right side is the outer wall of the duct. It can be seen that the turbulence intensities are total changed as θ increases. When θ is smaller than 360 deg, the variation of turbulence intensities with increasing θ is more obvious, while θ is greater than 360 deg, no significant change can be found.

4.4 Heat Transfer Differences Between Inner Wall and Outer Wall. Figure 6 shows the area averaged heat transfer coefficients on the inner and the outer walls for each half turn of the duct. The first point, which x is -0.25, is the heat transfer coefficient of a straight guide duct upstream of the curved duct. The blue line is the heat transfer coefficient calculated based on Sieder-Tate correlation. A good agreement of heat transfer coefficient between numerical result and the S-T correlation can be seen for the straight guide duct. Heat transfer coefficient on the outer wall is higher than that on the inner wall due to the effect of centrifugal force and secondary flow in the duct. It is also found that heat transfer on both the inner and the outer walls are larger than that of a straight duct (result of the S-T correlation). It indicates an overall heat transfer enhancement due to formation of secondary flow and increased turbulence intensity. A similar

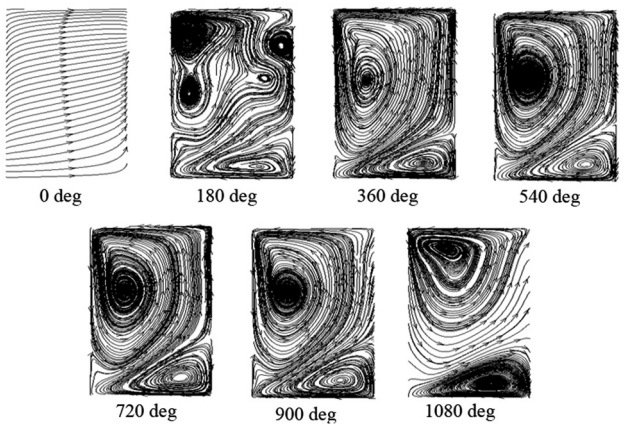

Fig. 3 Distribution of streamlines at varied cross sections ($\delta = 0.192$, $\lambda = 0.11$, and Re = 55,000)

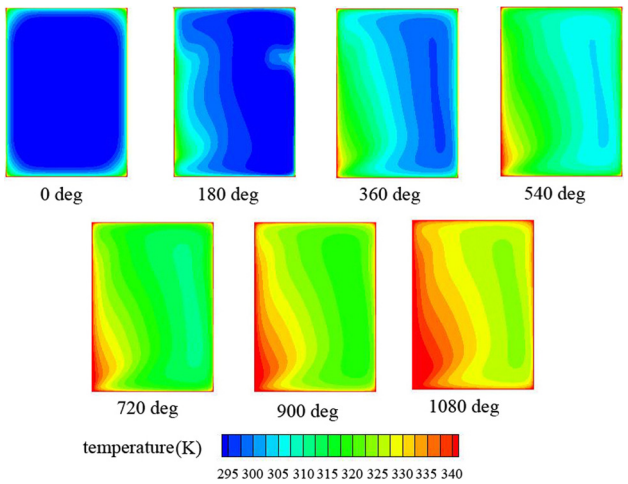

Fig. 4 Development of temperature field along the axial direction ($\delta = 0.192$, $\lambda = 0.11$, and Re = 55,000)

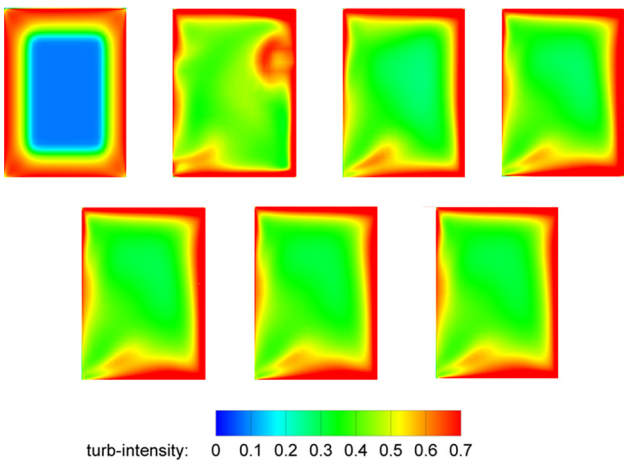

Fig. 5 Development of turbulence intensities distribution along the axial direction ($\delta = 0.192$, $\lambda = 0.11$, and Re = 55,000)

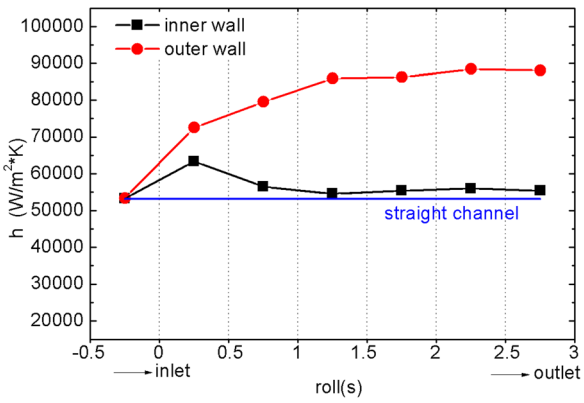

Fig. 6 Distribution of averaged heat transfer coefficients on the inner and outer walls ($\delta = 0.192$, $\lambda = 0.11$, and Re = 55000)

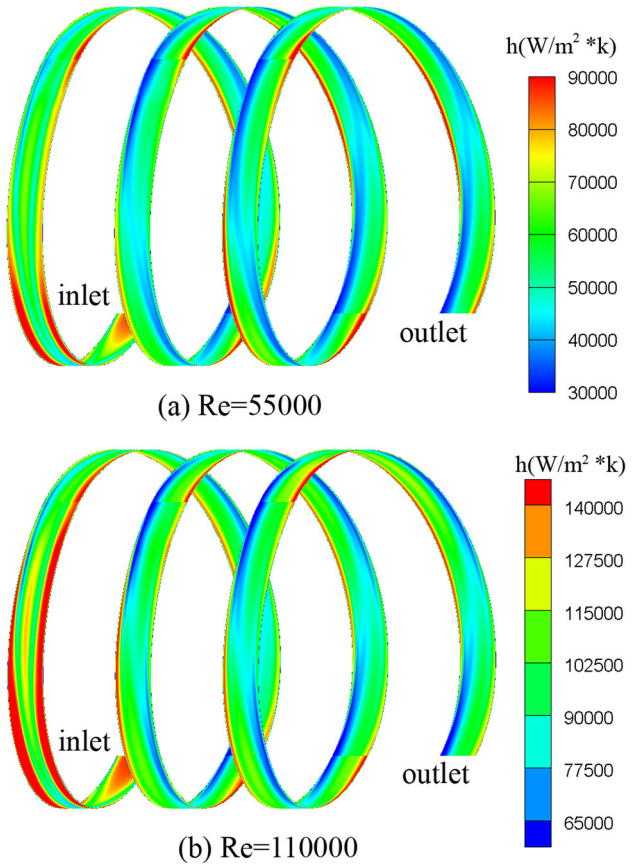

Fig. 7 Development of Nusselt numbers on the inner walls ($\delta = 0.192$ and $\lambda = 0.11$)

phenomenon has been found for heat transfer helical circular pipe [4]. Compare to the straight duct, heat transfer coefficient on the inner wall is 5% higher, and heat transfer coefficient on the outer wall is 60% higher.

4.5 Effect of Reynolds Number. It is worth noticing that most studies are focused on the outer wall of the channel where the heat transfer performance is normally enhanced by the secondary flow. Few heat transfer performance on the inner wall were discussed. So, in this paper, we focus on the inner wall that is usually the heat exchange surface for engine cooling applications.

For fixed δ and λ, development of nondimensional heat transfer coefficient on the inner wall are shown in Figs. 7(*a*) and 7(*b*) for two inlet Reynolds numbers. As shown in the figures, heat transfer coefficient increases with increasing of Reynolds number in overall. However, for the two Reynolds numbers, distributions of Nu at the same axial location are quite similar, only the quantity is changed. We can also see that the heat transfer coefficients distribution of the first turn from the inlet is quite different from the other turns. This might be the reason that the first turn is the developing region for the helical rectangular duct. And the h decreases with the increasing of the θ, it can be proved by the higher temperature near the inner wall with the increasing of the θ in Fig. 4. One can see from Table 3 that the friction factors decrease with increasing Reynolds numbers.

Table 3 The comparison of friction factors ($\delta = 0.192$ and $\lambda = 0.11$)

	Re = 55,000	Re = 110,000
f	0.0206	0.0173

Table 4 The comparison of friction factors ($\delta = 0.192$ and Re = 55,000)

	$\lambda = 0.11$	$\lambda = 0.22$
f	0.0206	0.0217

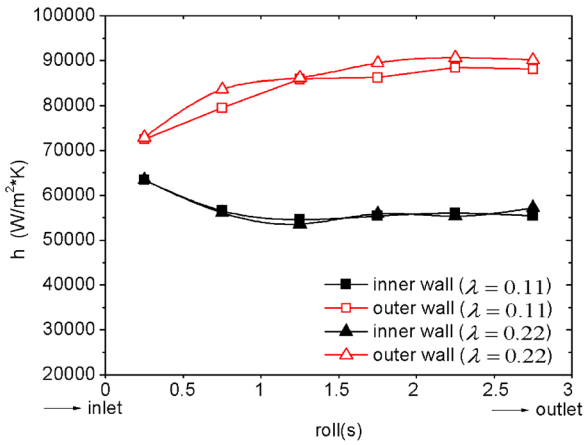

Fig. 8 Distribution of one-turn averaged heat transfer coefficients on the inner and outer walls of helical duct with two pitches ($\delta = 0.192$ and Re = 55,000)

4.6 Effects of Pitch. When δ and Reynolds number are given, changes of heat transfer coefficients on the inner and the outer walls are nearly the same with different pitches as plotted in Fig. 8. Note that differences are kept within 4%. The slight dependency of heat transfer properties on pitch is also found in other literatures [3,5]. On the other hand, the growing pitches increase the flow resistance, as shown in Table 4.

4.7 Effects of Curvature. Figure 9 shows comparison of averaged heat transfer coefficients on the inner and outer walls with different curvature with the same values of λ and Reynolds number. Xin and Ebadian [3] found that higher curvature results in higher averaged Nusselt number for a laminar helical pipe with curvature ratio from 0.0267 to 0.0884, while Wu et al. [5] found a different phenomena described by Xin and Ebadian [3] that the averaged Nusselt number decreases with increase of curvature for a turbulent flow in a helical coiled tube with curvature ratio form 0.1 to 0.3. For the present study, it is seen that difference of heat

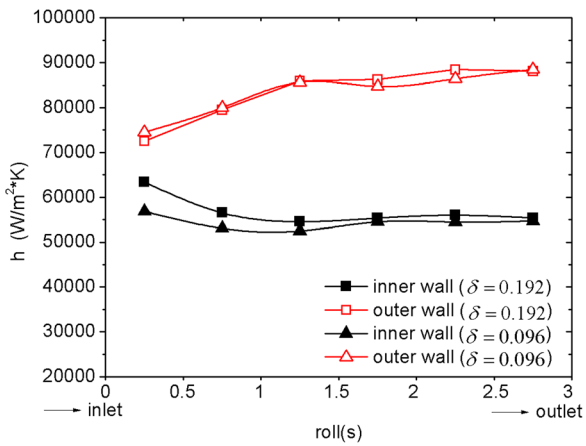

Fig. 9 Distribution of one-turn averaged heat transfer coefficients on the inner and outer walls of helical duct with two curvatures ($\lambda = 0.11$ and Re = 55,000)

Table 5 The comparison of friction factors ($\lambda = 0.11$, Re = 55,000)

	$\delta = 0.192$	$\delta = 0.096$
f	0.0206	0.0194

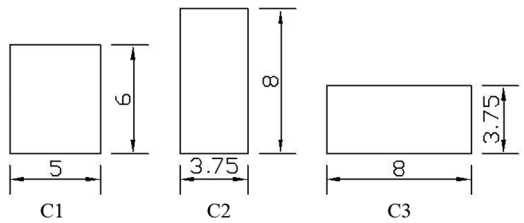

Fig. 10 The cross section of ducts (unit: mm)

transfer coefficient on the outer wall are small. However, variation of δ can affect heat transfer rate on the inner wall especially for the first turn from the entrance. This may be due to the fact that there exists a critical curvature ratio δ_{cri}, when $\delta \leq \delta_{cri}$, the averaged Nusselt number increases with the increment of curvature owing to the predominant contribution of turbulent disturbance, while $\delta \geq \delta_{cri}$, the opposite result does owing to the predominant contribution of secondary flow caused by the centrifugal force in helical coiled tube for turbulent flow. For a lower curvature, we get a lower friction factor, as shown in Table 5.

4.8 Effect of Parameters of Cross Section. Configurations of varied cross sections are shown in Fig. 10, and bottom wall is the inner wall of the helical duct. Areas of the three cross sections are the same, which means the inlet velocity and Reynolds number are nearly the same.

Figure 11 shows the comparison of averaged heat transfer coefficients on the inner and outer walls with different cross section configurations. One can see that configuration C2 with a large height-to-width ratio can enhance heat transfer coefficient on the inner wall strongly. While, heat transfer coefficients on the outer wall for the three configurations are nearly the same. Conversely, configuration C3 can reduce heat transfer rate on the outer wall remarkably, but does not affect heat transfer on the inner wall strongly. Figure 12 shows distribution of heat transfer coefficient

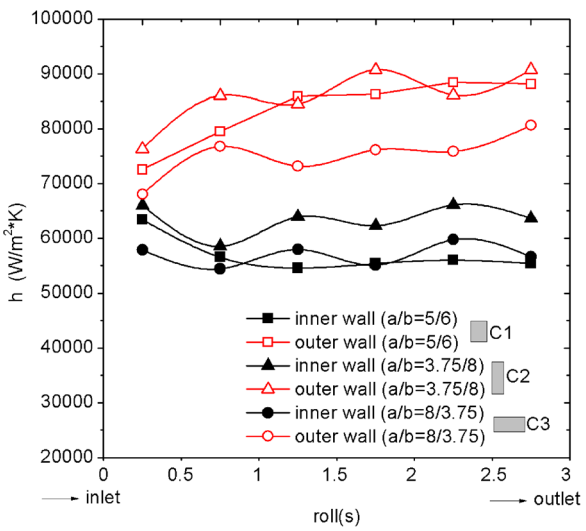

Fig. 11 Comparison of averaged heat transfer coefficients on the inner and outer walls for different duct configurations (Re = 55,000)

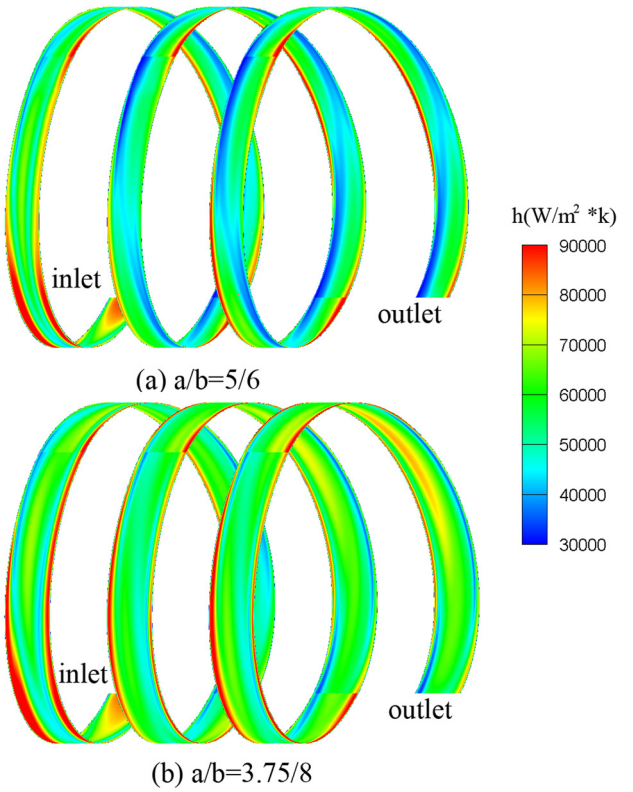

Fig. 12 The heat transfer coefficient distribution on the inner wall (Re = 55,000)

Table 6 The comparison of friction factors (Re = 55,000)

	C1	C2	C3
f	0.0206	0.0192	0.0211

on the inner wall with the configuration C1 and C2. There are local heat transfer valleys in configuration C1 caused by the secondary flow and shown as color blue. The region of heat transfer valley is much smaller in configuration C2. Therefore, when cross section area is given, making the height of the cooling duct larger can enhance heat transfer on both the inner and the outer walls. Therefore, when cross section area is given, making the height-to-width ratio of the duct larger can enhance heat transfer on both the inner and the outer walls. For the pressure loss, one can see the configuration C2 can get a much lower flow resistance coefficient, while configuration C3 get much higher pressure loss as Table 6.

5 Conclusions

In this paper, three-dimensional turbulent flow and convective heat transfer in helical rectangular ducts have been investigated numerically. The Navier–Stokes equations are solved with SST $k-\omega$ turbulence model and refined meshes in the near-wall region. The numerical results show the development of heat transfer and flow fields in the helical rectangular duct as well as the effect of flow and geometric parameters on heat transfer coefficients. It is found that heat transfer on the outer wall is enhanced due to the centrifugal effect. Significant secondary flow is observed in the cross sections along the axial direction and low-speed flow region is formed in the vicinity of the inner wall. Reynolds number can increase heat transfer coefficient in overall, but does not change its distribution. Larger curvature leads to higher heat transfer rate on the inner wall, but does not affect heat

transfer on the outer wall. Heat transfer coefficients on both inner and outer walls are nearly the same with different pitches. When area of cross section is kept the same, larger height can enhance heat transfer rate on the inner wall. When area of cross section is kept the same, larger height-to-width ratio can enhance heat transfer rate on the inner wall and reduce the pressure loss, which often act as the heat exchange surface in cooling system for rocket or scramjet. The present work is expected to provide some insights to the understanding of flow and convective heat transfer mechanisms of helical ducts.

Acknowledgment

The authors gratefully acknowledge the financial support of the National Natural Science Foundation of China (Nos. 11202218 and 11172309).

Nomenclature

a/b = width and height of the duct (mm)
h = heat transfer coefficient (W/m^2 K)
k = thermal conductivity (W/m K)
N = total number of cells
Nu = Nusselt number
p = coil pitch (mm)
R = curvature radius of the coil (mm)
Re = Reynolds number
u = bulk velocity (m/s)
δ = dimensionless curvature
θ = angle measured from the inlet plane of the coil
λ = dimensionless torsion
ρ = density (kg/m^3)

References

[1] Aly, W. I., Inaba, H., Haruki, N., and Horibe, A., 2006, "Drag, and Heat Transfer Reduction Phenomena of Drag-Reducing Surfactant Solutions in Straight and Helical Pipes," ASME J. Heat Transfer, **128**(8), pp. 800–810.
[2] Kao, H. C., 1987, "Torsion Effect on Fully Developed Flow in a Helical Pipe," J. Fluid Mech., **184**, pp. 335–356.
[3] Xin, R. C., and Ebadian, M. A., 1997, "The Effects of Prandtl Numbers on Local and Average Convective Heat Transfer Characteristics in Helical Pipes," ASME J. Heat Transfer, **119**(3), pp. 467–473.
[4] Ali, M. E., 2004, "Free Convection Heat Transfer From the Outer Surface of Vertically Oriented Helical Coils in Glycerol–Water Solution," Heat Mass Transfer, **40**(8), pp. 615–620.
[5] Wu, S. Y., Chen, S. J., Li, Y. R., and Li, L. J., 2009, "Numerical Investigation of Turbulent Flow, Heat Transfer and Entropy Generation in a Helical Coiled Tube With Larger Curvature Ratio," Heat Mass Transfer, **45**(5), pp. 569–578.
[6] Pizza, I. D., and Ciofalo, M., 2010, "Numerical Prediction of Turbulent Flow and Heat Transfer in Helical Coiled Pipes," Intern. J. Therm. Sci., **49**(1), pp. 653–663.
[7] Moawed, M., 2011, "Experimental Study of Forced Convection From Helical Coiled Tubes With Different Parameters," Energy Convers. Manage., **52**(2), pp. 1150–1156.
[8] Kaew-On, J., Nakkaew, S., and Wongwises, S., 2013, "Single-Phase Heat Transfer in the Straight and Helical Coiled Tubes," ASME Paper No. ICNMM2013-73109.
[9] Mandal, M. M., and Nigam, K. D. P., 2009, "Experimental Study on Pressure Drop and Heat Transfer of Turbulent Flow in Tube in Tube Helical Heat Exchanger," Ind. Eng. Chem. Res., **48**(20), pp. 9318–9324.
[10] Mandal, M. M., Kumar, V., and Nigam, K. D. P., 2010, "Augmentation of Heat Transfer Performance in Coiled Flow Inverter vis-à-vis Conventional Heat Exchanger," Chem. Eng. Sci., **65**(2), pp. 999–1007.
[11] Woike, M. R., and Willis, B. P., 2000, "Integrated Systems Testing for the Hypersonic Tunnel Facility," AIAA Paper No. 2000-2446.
[12] Traci, R. M., Farr, J. L., and Laganelli, T., 2002, "A Thermal Management Systems Model for the NASA GTX RBCC Concept," NASA, Technical Report No. NASA/CR-2002-211587.
[13] Naraghi, M. H., Pizzarelli, M., and Champagnon, R., 2011, "Heat Transfer Correlations for Transitional Coolant Flow From Curved to Straight Cooling Channel Sections," AIAA Paper No. 2011-5843.
[14] Thangam, S., and Hur, N., 1990, "Laminar Secondary Flows in Curved Rectangular Ducts," J. Fluid Mech., **217**(1), pp. 421–440.
[15] Bolinder, C. J., and Sunden, B., 1995, "Flow Visualization and LDV Measurements of Laminar Flow in a Helical Square Duct With Finite Pitch," Exp. Therm. Fluid Sci., **11**(4), pp. 348–363.
[16] Bolinder, C. J., 1996, "First and Higher-Order Effects of Curvature and Torsion on the Flow in a Helical Rectangular Duct," J. Fluid Mech., **314**, pp. 113–138.
[17] Zabielski, L., and Mestel, A. J., 1998, "Steady Flow a Helically Symmetric Pipe," J. Fluid Mech., **370**, pp. 297–320.
[18] Zabielski, L., and Mestel, A., 2005, "Kinematic Dynamo Action in a Helical Pipe," J. Fluid Mech., **535**, pp. 347–367.
[19] Sakalis, V. D., Hatzikonstantinou, P. M., and Papadopoulos, P. K., 2005, "Numerical Procedure for the Laminar Developed Flow in a Helical Square Duct," ASME J. Fluids Eng., **127**(1), pp. 136–148.
[20] Egner, M. W., and Burmeister, L. C., 2005, "Heat Transfer for Laminar Flow in Spiral Ducts of Rectangular Cross Section," ASME J. Heat Transfer, **127**(3), pp. 352–356.
[21] Kurnia, J. C., Sasmito, A. P., and Mujumdar, A. S., 2011, "Evaluation of the Heat Transfer Performance of Helical Coils of Non-Circular Tubes," J. Zhejiang Univ. Sci. A, **12**(1), pp. 63–70.
[22] Mori, Y., Uchida, Y., and Ukon, T., 1971, "Forced Convective Heat Transfer in a Curved Channel With a Square Cross Section," Int. J. Heat Mass Transfer, **14**(3), pp. 1787–1805.
[23] Srinivasan, P. S., Nandapurkar, S., and Holland, F. A., 1970, "Friction Factor for Coils," Trans. Inst. Chem. Eng., **48**(6), pp. 156–161.